AMERICAN SOCIETY FOR MICROBIOLOGY | mSystems

Editor's Pick | Human Microbiome | Research Article

Metagenome-assembled genomes reveal microbial signatures and metabolic pathways linked to coronary artery disease

Soomin Lee,[1] Shahbaz Raza,[1] Eun-Ju Lee,[1] Yoosoo Chang,[1,2,3] Seungho Ryu,[1,2,3] Hyung-Lae Kim,[4] Si-Hyuck Kang,[5,6] Han-Na Kim[1,7]

AUTHOR AFFILIATIONS See affiliation list on p. 14.

Downloaded from https://journals.asm.org/journal/msystems on 27 May 2026 by 203.255.190.49.

ABSTRACT Gut microbiota has emerged as a critical factor influencing cardiovascular disease (CVD) risk, particularly coronary artery disease (CAD) development. Using fecal metagenomic shotgun sequencing, we investigated gut microbiota signatures associated with CAD and provided strain-resolved insights through metagenome-assembled genome (MAG) reconstruction. We analyzed 14 patients with CAD and 28 propensity score-matched healthy controls. Differential abundance analysis identified 15 CAD-associated bacterial species. Members of the *Lachnospiraceae* family, previously associated with trimethylamine-N-oxide production, were significantly enriched in patients with CAD. Conversely, short-chain fatty acid-producing bacteria *Slackia isoflavoniconvertens* and *Faecalibacterium prausnitzii* were depleted, suggesting a potential contribution to gut-mediated inflammation and metabolic dysregulation. Metabolic pathway analysis revealed significant urea cycle and L-citrulline biosynthesis enrichment in CAD cases, with *Alistipes* and *Coprococcus* as key contributors. Among predicted metabolites, inosine, which is implicated in coronary artery relaxation, was elevated in patients with CAD, whereas C18:0e MAG and α-muricholate were depleted. A random forest model achieved a mean AUC of 0.89 for CAD classification, with improved performance when integrating microbial taxa and metabolites. CAD-derived MAGs showed metabolic signatures linked to inflammatory dysbiosis and cardiovascular dysfunction, such as enriched N_2 fixation and sulfite reduction. Strain-resolved comparative genomic analysis of MAGs revealed distinctive functional characteristics between CAD-derived and control-derived strains of *Akkermansia muciniphila* and *Megamonas fumiformis*. *F. prausnitzii* MAG from the control group carried non-trimethylamine-producing gene, *mtxB*, suggesting its potential protective role in CAD pathophysiology. These findings provide insights into gut microbial alterations in CAD and highlight potential targets for microbiome-based therapeutic interventions to reduce CVD risk.

IMPORTANCE Gut microbiota plays a pivotal role in cardiovascular disease; however, its specific contribution to coronary artery disease (CAD) remains underexplored. This study identified distinct microbial signatures associated with CAD, including the enrichment of pro-inflammatory bacterial taxa and depletion of short-chain fatty acid-producing bacteria, which may contribute to systemic inflammation and metabolic dysregulation. Perturbations in key pathways, such as the urea cycle and glycolysis, suggest metabolic links between the gut microbiota and CAD. Additionally, the metagenome-assembled genome-based analysis revealed strain-resolved functional heterogeneity that shapes host-microbe interactions and may contribute to CAD pathophysiology. These findings provide novel insights into gut dysbiosis in CAD and highlight the potential of microbiome-targeted therapeutic strategies in precision medicine.

KEYWORDS coronary artery disease, cardiovascular disease, gut microbiome, shotgun metagenomics, metagenome-assembled genome

Editor Ying Zhang, University of Rhode Island, Kingston, Rhode Island, USA

Address correspondence to Han-Na Kim, hanna147942@gmail.com.

The authors declare no conflict of interest.

See the funding table on p. 14.

Received 27 June 2025
Accepted 27 September 2025
Published 6 November 2025

Copyright © 2025 Lee et al. This is an open-access article distributed under the terms of the Creative Commons Attribution 4.0 International license.

Downloaded from https://journals.asm.org/journal/msystems on 27 May 2026 by 203.255.190.49.

Cardiovascular disease (CVD) is a leading cause of global mortality and morbidity, with coronary artery disease (CAD) representing a prevalent form of CVD characterized by myocardial dysfunction and lesions due to coronary artery stenosis and inadequate blood supply (1). Approximately half of the adults in the USA suffer from CVD, for ~25% of which it is fatal (1). In South Korea, CVD is the second leading cause of death among adults after cancer (2). Although genetic and environmental factors contribute to CAD, emerging research highlights the pivotal role of the gut microbiota in disease progression via its impact on systemic inflammation, lipid metabolism, and atherosclerosis (3). However, the specific microbial taxa and functional pathways involved remain poorly understood and require further investigation into their mechanistic roles.

Gut microbiota-derived metabolites, particularly trimethylamine-N-oxide (TMAO), have been implicated in CAD pathogenesis by linking dietary choline metabolism to systemic inflammation, endothelial dysfunction, and progression (4). The microbial conversion of dietary choline and L-carnitine into trimethylamine (TMA), followed by hepatic oxidation to TMAO, promotes vascular inflammation, platelet hyperreactivity, and foam cell formation, contributing to plaque development and cardiovascular risk (3, 5). In addition to TMAO, the gut microbiota modulates lipid metabolism, bile acid transformation, and short-chain fatty acid (SCFA) production, influencing host metabolism and immune responses relevant to CAD (6).

Emerging evidence suggests that microbiota-based interventions may help to modulate cardiovascular risk. A randomized controlled trial demonstrated that probiotic supplementation with *Lactobacillus rhamnosus* significantly reduced systemic inflammation, metabolic endotoxemia, and inflammatory cytokine levels in patients (7). Similarly, dietary interventions targeting gut microbiota modifications have shown potential in improving lipid metabolism and vascular function, emphasizing the therapeutic relevance of microbiome modulation in cardiovascular health (8).

Despite these insights, CAD-associated microbiota remained incompletely characterized, especially at the species and strain levels. Although 16S rRNA sequencing has revealed broad compositional shifts, it lacks species- and strain-level functional insights (9). In contrast, shotgun metagenomics enables species-level classification and metabolic pathway reconstruction (10), providing a more comprehensive view of microbial contributions to CAD. A key advancement is the reconstruction of metagenome-assembled genomes (MAGs), which allows *de novo* assembly of microbial genomes, including those of uncultured and low-abundance microbes. Thus, they offer deep insights into microbial diversity and functional capabilities (11).

In this study, we used shotgun metagenomics to comprehensively profile the gut microbiomes of patients with CAD and healthy controls by examining both taxonomic and functional alterations. Our objectives were to (i) identify differences in microbial composition between patients with CAD and healthy individuals, (ii) characterize metabolic pathways and predict gut metabolites linked to CAD, and (iii) reconstruct MAGs to uncover uncharacterized genomes associated with CAD. By emphasizing strain-level taxonomy and metabolic functions, this study extends beyond traditional taxonomic profiling to explore how microbial functions and metabolic interactions contribute to the pathophysiology of CAD.

RESULTS

Basic characteristics of participants

After propensity score matching (PSM), 42 participants were included in the final analysis, comprising 14 patients with CAD and 28 matched controls (Table 1). The mean age of participants was 53.3 years (range: 40–70 years), and the mean body mass index (BMI) was 24.5 (range: 19.0–30.7). Three of the participants were female. Before PSM, age and high-sensitivity C-reactive protein levels differed significantly between the groups (*t*-test, $P < 0.05$; Table S1, Fig. S1); however, these differences were no longer significant after PSM, confirming the balance achieved through the matching process (Table 1).

Downloaded from https://journals.asm.org/journal/msystems on 27 May 2026 by 203.255.190.49.

TABLE 1 Basic characteristics of all the participants after propensity score matching[a]

Characteristic	Overall (*n* = 42)	Case (*n* = 14)	Control (*n* = 28)	*P*-value
Sex (%)				
Female	3	1 (7.2%)	2 (7.1%)	0.579
Male	39	13 (92.8%)	26 (92.9%)	
Age (years), mean ± SD	53.3 ± 9.2	52.4 ± 9.5	53.7 ± 9.2	0.68
BMI (kg/m), mean ± SD	24.7 ± 3.0	24.7 ± 3.0	24.4 ± 3.0	0.729
TG (mg/dL), mean ± SD	128.4 ± 53.7	109.5 ± 27.6	136.9 ± 60.5	0.051
HDL-C (mg/dL), mean ± SD	54.3 ± 12.5	51.5 ± 12.4	55.6 ± 12.6	0.326
Glucose (mg/dL), mean ± SD	96.8 ± 9.5	97.2 ± 11.1	96.6 ± 8.9	0.842
SBP (mmHg), mean ± SD	112.8 ± 9.6	110.8 ± 9.7	113.6 ± 9.7	0.395
DBP (mmHg), mean ± SD	74.0 ± 7.2	72.7 ± 7.0	74.6 ± 7.4	0.439
HCRP (mg/L)	0.05 ± 0.04	0.04 ± 0.02	0.05 ± 0.04	0.317
CRP (mg/L)	0.05 ± 0.05	0.05 ± 0.04	0.06 ± 0.05	0.712

[a]BMI, body mass index; TG, triglyceride; HDL-C, high-density lipoprotein cholesterol; SBP, systolic blood pressure; DBP, diastolic blood pressure; HCRP, high-sensitivity C-reactive protein; CRP, C-reactive protein.

Shotgun metagenomic sequencing yielded an average of 45,844,546 raw reads per participant, of which 39,651,636 remained after host DNA was removed and were used for further analyses (Table S2).

Microbial community structure in patients with CAD

Among 42 participants, 520 bacterial species were identified. The most prevalent species across all individuals were *Prevotella copri* (recently renamed to *Segatella copri*, 14.37%), *Phocaeicola coprocola* (4.78%), and *Phocaeicola vulgatus* (4.44%; Table S3). Microbial diversity analysis revealed no significant differences in alpha diversity between patients with CAD and controls, as assessed using the Chao, Simpson, Shannon, and Pielou indices (Wilcoxon rank-sum test, $P > 0.05$; Fig. S2A). Similarly, Bray–Curtis distance-based beta diversity did not show significant differences between groups (permutational multivariate analysis of variance, PERMANOVA, $P > 0.05$; Fig. S2B).

Differential abundance analysis identified 15 bacterial species with significantly different relative abundances between patients with CAD and controls (linear regression model, $P < 0.05$). Among these, seven bacterial species, including *CAG-303*

TABLE 2 Differentially abundant bacterial species in the case and control groups[a]

Taxonomy	Coefficient	Relative abundance		*P*-value
		Case	Control	
p__Firmicutes_A;c__Clostridia;o__Lachnospirales;f__Lachnospiraceae;g__*CAG-303*;s__*CAG-303 sp000437755*	3.262	0.162	0.003	0.004
p__Actinobacteriota;c__Coriobacteriia;o__Coriobacteriales;f__Eggerthellaceae;g__*Slackia_A*;s__*Slackia_A isoflavoniconvertens*	−2.017	0.000	0.050	0.013
p__Firmicutes_A;c__Clostridia;o__Lachnospirales;f__Lachnospiraceae;g__*AM51-8*;s__*AM51-8 sp003478275*	2.724	0.340	0.055	0.015
p__Firmicutes_A;c__Clostridia;o__Oscillospirales;f__Ruminococcaceae;g__*Faecalibacterium*;s__*Faecalibacterium prausnitzii*	−2.473	0.616	1.744	0.024
p__Firmicutes;c__Bacilli;o__Erysipelotrichales;f__Coprobacillaceae;g__*Catenibacterium*;s__*Catenibacterium sp000437715*	−2.493	0.034	0.209	0.024
p__Firmicutes_A;c__Clostridia;o__Oscillospirales;f__Oscillospiraceae;g__CAG-83;s__*CAG-83 sp900757415*	−1.052	0	0.014	0.029
p__Firmicutes;c__Bacilli;o__Erysipelotrichales;f__Coprobacillaceae;g__*Faecalibacillus*;s__*Faecalibacillus intestinalis*	1.972	0.072	0.017	0.031
p__Firmicutes_A;c__Clostridia;o__Oscillospirales;f__Acutalibacteraceae;g__*UBA737*;s__*UBA737 sp002431945*	1.300	0.234	0.000	0.033
p__Bacteroidota;c__Bacteroidia;o__Bacteroidales;f__Bacteroidaceae;g__*Prevotella*;s__*Prevotella copri_A*	−3.708	3.34E−04	4.15E+00	0.035
p__Firmicutes_A;c__Clostridia;o__Lachnospirales;f__Lachnospiraceae;g__*Lachnospira*;s__*Lachnospira eligens_A*	−3.036	0.047	0.429	0.039
p__Firmicutes;c__Bacilli;o__Erysipelotrichales;f__Erysipelotrichaceae;g__*Holdemanella*;s__*Holdemanella porci*	−2.541	0.020	0.146	0.041
p__Firmicutes_A;c__Clostridia;o__Oscillospirales;f__Oscillospiraceae;g__*Lawsonibacter*;s__*Lawsonibacter sp014287875*	−1.199	0.002	0.022	0.041
p__Firmicutes_A;c__Clostridia;o__UBA1381;f__UBA1381;g__*CAG-41*;s__*CAG-41 sp900066215*	3.886	0.493	0.236	0.042
p__Firmicutes_A;c__Clostridia;o__Lachnospirales;f__Lachnospiraceae;g__*Ventrimonas*;s__*Ventrimonas sp900538475*	1.850	0.078	0.005	0.043
p__Firmicutes_A;c__Clostridia;o__Oscillospirales;f__UBA644;g__*UBA644*;s__*UBA644 sp900547165*	1.086	4.03E−03	3.75E−04	0.046

[a]*P*-values were generated from the generalized linear model using Microbiome Multivariable Association with Linear Model 2 (MaAsLin2) between the two groups. Significantly different species were also observed ($P < 0.05$, linear regression model). The coefficients represent the direction of significance in each case. Negative coefficient values indicate higher abundance in the control group.

sp000437755, *AM51-8 sp003478275*, *Ventrimonas sp900538475*, and *UBA644 sp900547165*, were significantly more abundant in the CAD cases (Table 2). In contrast, eight bacterial species, including *Slackia_A isoflavoniconvertens*, *Faecalibacterium prausnitzii*, *Catenibacterium sp000437715*, *Prevotella copri_A*, *Lachnospira eligens_A*, and *Holdemanella porci*, were significantly depleted in CAD cases compared with those in the control group. These findings suggest potential taxonomic shifts in the gut microbiome of patients with CAD, characterized by an increased abundance of certain bacterial taxa and depletion of SCFA-producing species.

Downloaded from https://journals.asm.org/journal/msystems on 27 May 2026 by 203.255.190.49.



FIG 1 Metabolic pathways associated with coronary artery disease (CAD). (A) Bubble plot for differentially abundant pathways between case and control. *P*-values were calculated from differential abundance analysis with the Microbiome Multivariable Association with Linear Models 2 (MaAsLin2). The size of the bubble is based on *P*-values, where a larger size represents higher significance (lower *P*-value). The color of the bubble is based on its abundance in the case or control groups. Red color indicates higher abundance in cases, and blue represents higher abundance in the control group. (B) Contribution of bacterial genera in the abundance of the urea cycle pathway, (C) L-citrulline biosynthesis, (D) glycolysis III (from glucose), (E) CDP-diacylglycerol biosynthesis I, (F) CDP-diacylglycerol biosynthesis II, and (G) L-isoleucine biosynthesis III. The plot was generated with the HUMAnN3 bar graph plugin. We used the options of Bray–Curtis, and samples were sorted based on metadata.

Downloaded from https://journals.asm.org/journal/msystems on 27 May 2026 by 203.255.190.49.

Functional signature of gut microbiota in patients with CAD

Functional pathway analysis identified 10 MetaCyc metabolic pathways that differed significantly between patients with CAD and controls (linear regression model, $P < 0.05$; Fig. 1A). Among these, seven pathways, including the urea cycle, L-citrulline biosynthesis, glycolysis III (from glucose), and CDP-diacylglycerol biosynthesis, were significantly enriched in patients with CAD. Conversely, three metabolic pathways, including L-isoleucine biosynthesis III and the superpathway of branched-chain amino acid (BCAA) biosynthesis, were significantly depleted in patients with CAD.

To quantify the functional contributions of bacterial communities, we utilized the HUMAnN3 framework and stratified these functions based on the contributing species, referred to as "contributional diversity" of the function (12). In the urea cycle pathway, the predominant contributing genera were *Alistipes* and *Flavonifractor* (Fig. 1B). At the species level, *Alistipes finegoldii* and *Flavonifractor plautii* were the primary contributors, whereas *Alistipes onderdonkii* was detected exclusively in patients with CAD, and *Coprococcus catus* mainly contributed to controls (Fig. S3). In the L-citrulline biosynthesis pathway, *Alistipes*, *Escherichia,* and *Klebsiella* were the predominant contributors. *Escherichia* was enriched in CAD patients, whereas *Coprococcus* and *Klebsiella* were more prevalent in the control group (Fig. 1C). In glycolysis III (from glucose), *Escherichia*, *Klebsiella*, and *Bacteroides* were the predominant contributors (Fig. 1D). The predominant contributors to CDP-diacylglycerol biosynthesis I and II were *Bacteroides*, *Faecalibacterium*, and *Escherichia* (Fig. 1E and F). In the L-isoleucine biosynthesis III pathway, the major contributors were *Prevotella* and *Bacteroides* across all participants (Fig. 1G).

To better characterize the functional shifts in the gut microbiome associated with CAD, we analyzed the microbiota metabolic potential and anaerobic fermentation capacity using the human gut metabolic module (GMM) (13). Seven GMMs were significantly enriched in patients with CAD (linear regression model, $P < 0.05$; Fig. 2). Specifically, three amino acid degradation-associated modules (aspartate, serine, and arginine degradation) and four carbohydrate degradation-associated modules (galactose, lactose, xylose, and pectin degradation) were significantly enriched in patients with CAD.

Using UniRef90 profiles from HUMAnN3, we predicted the gut microbial metabolites and identified 80 metabolites. Of these, three metabolites differed significantly between patients with CAD and controls (linear regression model, $P < 0.05$; Table 3). Inosine was significantly elevated in patients with CAD, whereas C18:0e MAG and alpha-muricholate were significantly depleted in patients with CAD compared with those in the controls.

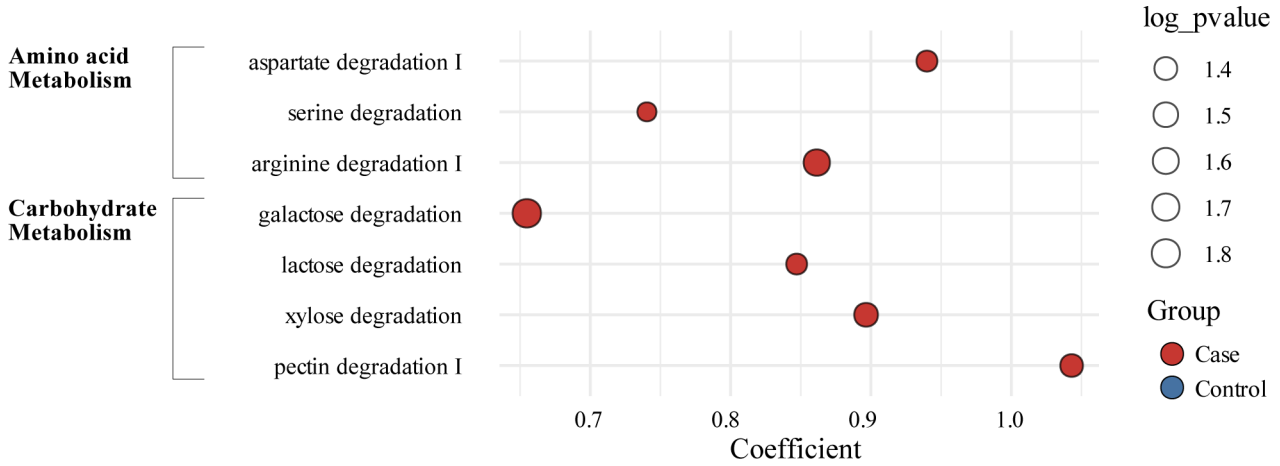


FIG 2 Human gut metabolic modules associated with CAD. Bubble plot for differentially abundant gut metabolic modules (GMMs) between the case and control groups. *P*-values were calculated from differential abundance analysis with MaAsLin2. The size of the bubble is based on *P*-values, where a larger size represents higher significance (lower *P*-value). Red color indicates higher abundance in cases, and blue represents higher abundance in the control group.

TABLE 3 Differentially abundant predicted metabolites in the case and control groups[a]

Metabolite	Coefficient	Relative abundance (%)		*P*-value
		Case	Control	
Inosine	0.267	0.009	0.008	2.01E−04
C18:0e MAG	−0.074	0.006	0.006	2.26E−02
Alpha-muricholate	−0.407	0.032	0.042	3.65E−02

[a]*P*-values were generated from the linear regression model using MaAsLin2 between the two groups. Significantly different species were identified. Positive coefficient values indicate higher abundance in the cases compared with controls.

In addition, we examined the relative abundance of bacterial genes encoding enzymes involved in TMA synthesis, including *CutC*, *Grdl,* and *MttB* (Fig. S4). No significant differences were observed between patients with CAD and controls ($P > 0.05$, Wilcoxon rank-sum test).

Prediction models for CAD

To evaluate the predictive potential of the gut microbiota in distinguishing CAD cases from controls, we developed a random forest classification model using differentially abundant bacterial species and metabolites. A classification model based on bacterial species achieved a mean area under the curve (AUC) of 0.79 (95% confidence interval [CI]: 0.47%–1.00%; Fig. 3A), with *AM51-8 sp003478275*, *F. prausnitzii*, and *F. intestinalis* as the top-ranking predictors (Fig. 3B). Similarly, the metabolites-based model yielded a mean AUC of 0.78 (95% CI: 0.47%–1.00%; Fig. 3C), with inosine showing the highest feature importance, followed by alpha-muricholate and C18:0e MAG (Fig. 3D). When bacterial taxa and metabolites were combined, the predictive performance improved, resulting in a mean AUC of 0.89 (95% CI: 0.59%–1.00%; Fig. 3E), highlighting the complementary predictive value of taxonomic and metabolic features. In this combined model, inosine, alpha-muricholate, *F. prausnitzii*, C18:0e MAG, and *AM51-8 sp003478275* were highly important (Fig. 3F). Receiver operating characteristic (ROC) curve analysis indicated that integrating both microbial taxa with metabolites enhanced the predictive accuracy of CAD classification compared with models utilizing a single feature type.

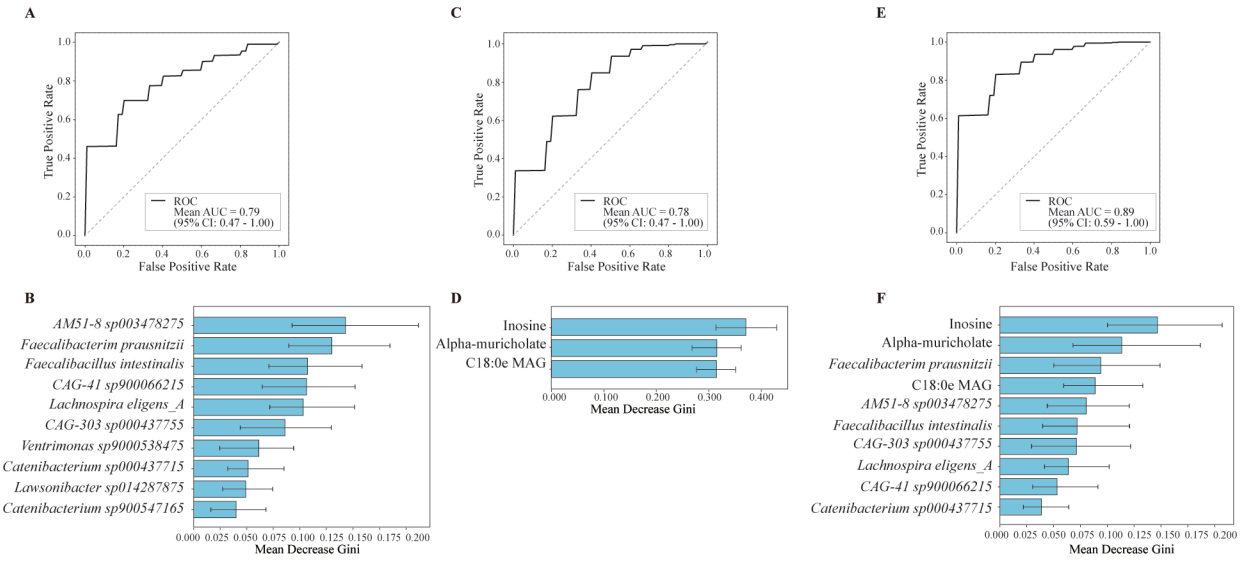


FIG 3 Random forest classification models to distinguish CAD cases from controls. Receiver operating characteristic (ROC) curves based on differentially abundant (A) bacterial species, (C) predicted microbial metabolites, and (E) a combined feature set of both. Feature importance ranked by mean decrease Gini (MDG) for each model, corresponding to (B) species-only, (D) metabolite-only, and (F) combined models. Area under the curve (AUC) and MDG value were evaluated using fivefold cross-validation repeated 50 times. The results are summarized as mean values with 95% confidence intervals across iterations.

Downloaded from https://journals.asm.org/journal/msystems on 27 May 2026 by 203.255.190.49.

Downloaded from https://journals.asm.org/journal/msystems on 27 May 2026 by 203.255.190.49.

Identification of MAGs in patients with CAD

MAGs were reconstructed separately for CAD cases and controls using co-assembled contigs (Table S4). A total of 31 bins were reconstructed, with 17 originating from CAD cases and 14 from control participants. In total, 25 distinct MAG species were identified, including six shared between both groups, 11 species found only in CAD cases, and eight species found only in the control group. The six MAGs found in both groups were *Brachyspira aalborgi*, *Megamonas funiformis*, *Sutterella wadsworthensis_A*, *Sutterella wadsworthensis*, *Akkermansia muciniphila,* and *PeH17 sp000435055*. Taxonomic classifications and relative abundances of all MAGs identified in CAD cases and controls are provided in Tables S5 and S6. Among the 25 species identified from co-assembly MAGs, by excluding the six species shared between CAD cases and controls, 18 species overlapped with those detected using MetaPhlAn4, a reference-based taxonomic profiling tool (Fig. S5A).

In addition to the co-assembly approach, we performed individual assemblies for each sample, which resulted in the reconstruction of 326 bacterial MAGs (Table S7). After dereplication at 95% average nucleotide identity (ANI), a total of 144 distinct species-level MAGs were identified through taxonomic classification (Table S8). Among the 25 MAG species identified from co-assembly, 24 MAG species were identified in the individual-assembly-based MAG set, except for *Paraprevotella clara*. Instead, a closely related genome, *Paraprevotella xylaniphila*, which shared 92.62% ANI with *P. clara*, was identified in the individual assembly. Among the 144 MAG species identified through individual assemblies, 96 species overlapped with those detected using MetaPhlAn4 (Fig. S5B). This overlap suggests that a substantial proportion of the MAGs reconstructed

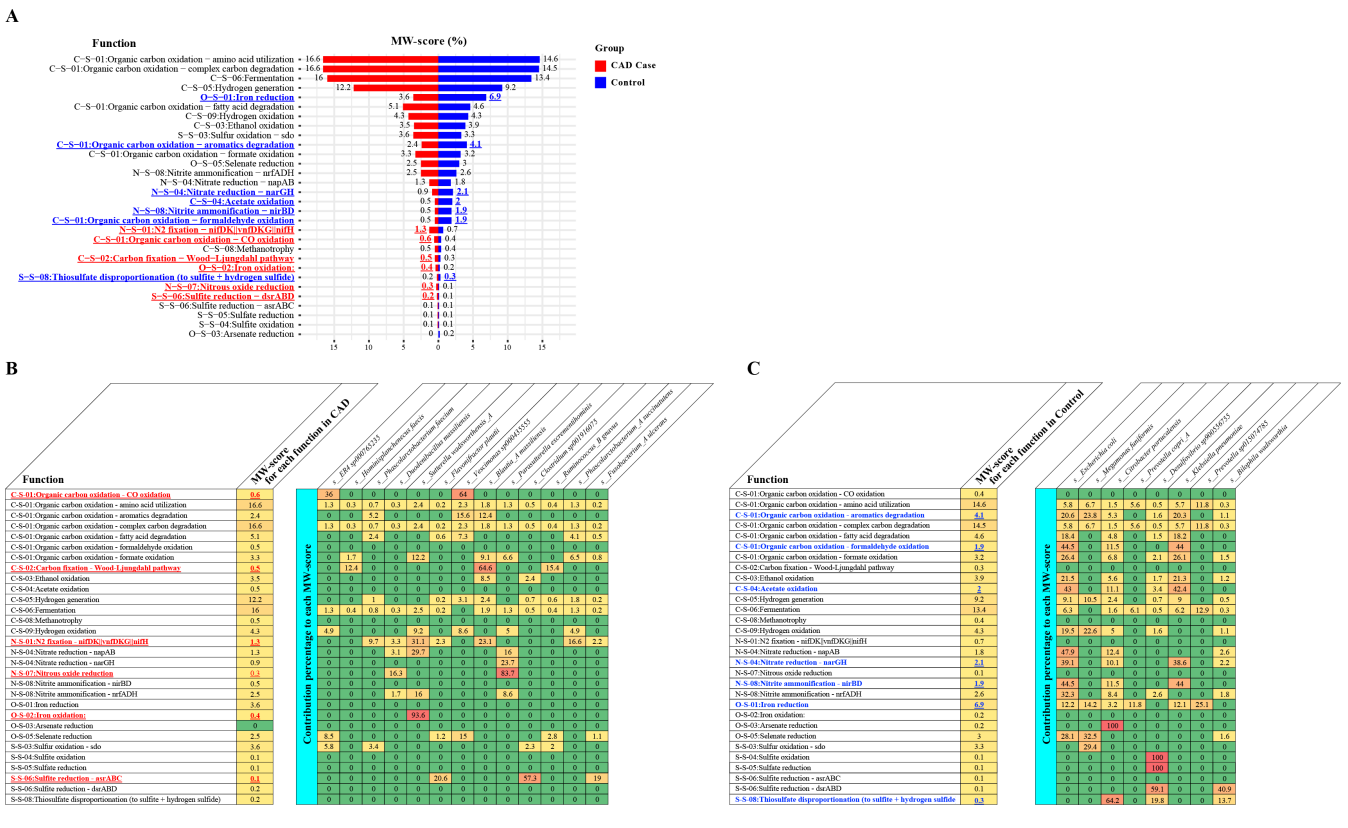


FIG 4 Community-scale metabolic profiling of MAGs using METABOLIC (v4.0). (A) Comparison of metabolic weight scores (MW-scores) of individual assembly MAGs between case and control groups. MW-scores represent the proportion of each metabolic function within the total functional capacity of the microbial community. Heatmaps showing species-level contributions to each metabolic function in CAD-derived MAGs (B) and control-derived MAGs (C), calculated using the METABOLIC-C.pl function.

in this study correspond to previously characterized microbial species, whereas the remaining MAGs may represent less well-characterized or novel taxa.

To assess the potential metabolic interactions within microbial communities, we performed community-scale metabolic profiling of MAGs using metabolic weight scores (MW-scores) (14), which quantify the relative proportion of each metabolic function within the overall functional capacity of the microbial community. In the analysis based on MAGs reconstructed from individual assemblies, MAGs from CAD cases exhibited more than 1.5-fold higher MW-scores for N_2 fixation, CO oxidation, carbon fixation, iron oxidation, nitrous oxide reduction, and sulfite reduction (Fig. 4A), with *Suterella wadsworthensis, Phascolarctobacterium succinatutens*, and *Clostridium sp001916075* serving as the predominant contributors (Fig. 4B). In contrast, controls-derived individual MAGs showed higher MW scores for aromatic degradation, formaldehyde oxidation, acetate oxidation, nitrate reduction, nitrite ammonification, iron reduction, and thiosulfate disproportionation (Fig. 4C), with major contributors, including *M. funiformis*, *Prevotella copri*, *S. wadsworthensis*, and *Bilophila wadsworthia*. Notably, N_2 fixation and sulfite reduction were consistently enriched in CAD-derived co-assembly MAGs. Conversely, iron reduction, aromatic degradation, and nitrite ammonification were elevated in control-derived co-assembly MAGs as shown from individual MAGs (Fig. S6).

Furthermore, to assess the genome-scale metabolic potential of MAGs, we examined the functional genes associated with DRAM-annotated metabolic modules (15), lipid metabolism (KEGG: 09103), CVD (KEGG: 09166), and TMA-metabolism (Fig. S7; Table S9). CAD-derived MAGs carried several genes related to ether lipid metabolism (ko00565) or steroid biosynthesis (ko00100/ko00140, Fig. S7A). The TMA-producing gene, *cutC*, was identified from nine MAGs, including six *A. hadrus* MAGs (Case_CM_28, Control_IM_KR_0042_concoct_bin.62, etc.), two *Desulfovibrio sp900556755* MAGs, and one *Bilophila wadsworthia* MAG. Another TMA-producing gene, *cntA/yeaW*, was identified from 10 *M. fumiformis* MAGs (Case_CM_45, Control_CM_39, Control_IM_KR_0032_concoct_bin.15, etc.), one *Klebsiella pneumoniae* MAG, and one *Escherichia coli* MAG. The *mttB (pyl)*, non-TMA-producing gene, was identified from three *Phocaeicola* species MAGs from both CAD and control groups. Another non-TMA-producing gene, *mtxB*, was identified from *Phocaeicola plebeius_A* and *F. prausnitzii* MAGs from only the control group.

To evaluate the metabolic features and genetic diversity of the MAGs identified in this study against reference genomes, we conducted a strain-level comparative genomic analysis of four species identified in both case and control MAGs (*B. aalborgi*, *M. fumiformis*, *A. muciniphila*, and *S. wadsworthensis*) using a public database. The control-derived *A. muciniphila* MAGs, control-derived MAGs, Control_CM_12, Control_IM_KR_0033_metabat2_bin.50, and Control_IM_KR_0039_concoct_bin.28, carried functional modules for arabinan and xyloglycan degradation, compared with the CAD-derived *A. muciniphila* MAGs, Case_CM_16 and Case_IM_KR0014_metabat2_bin.41 (Fig. S8). The CAD-derived *M. fumiformis* MAG, Case_CM_45, displayed carriage of metabolic modules related to methanogenesis, mercury reduction, acetate conversion, and lipid metabolism compared with those from eight control-derived MAGs, including Control_CM_39, Control_IM_KR_0033_concoct_bin.53, and Control_IM_KR_0031_metabat2_bin.41 (Fig. S9). No significant differences were found between the CAD and control MAGs in terms of *B. aalborgi* and *S. wadsworthensis* (Fig. S10 and S11).

DISCUSSION

This study provides a comprehensive analysis of gut microbiota composition, metabolic pathways, predicted microbial metabolites, and MAGs in individuals with CAD using shotgun metagenomic sequencing. These findings contribute to our understanding of gut microbial alterations in patients with CAD and offer potential implications for microbiome-based therapeutic interventions. Notably, high AUC values in predictive models indicate that gut microbial markers may be clinically relevant for noninvasive CAD risk stratification. However, further validation in larger cohorts and longitudinal

Downloaded from https://journals.asm.org/journal/msystems on 27 May 2026 by 203.255.190.49.

studies is required to confirm these findings and assess their applicability in clinical settings.

We identified 15 bacterial species with differential abundance between patients with CAD and controls, underscoring the potential taxonomic shifts associated with CAD. Several members of the Lachnospiraceae family were significantly enriched in the CAD cases, whereas *Lachnospira eligens A* was depleted. Previous studies have reported a reduction in Lachnospiraceae in CAD, which is often associated with lower SCFA production (16) and increased TMAO levels (3), both of which contribute to the progression of atherosclerosis. However, our findings suggest an enrichment of distinct Lachnospiraceae taxa, indicating a more nuanced role for this family in CAD. In contrast, well-characterized SCFA-producing bacteria, such as *F. prausnitzii*, *Catenibacterium* spp., and *Holdemanella* spp., were consistently depleted in CAD. *F. prausnitzii*, a well-known butyrate producer, plays a key role in maintaining intestinal barrier integrity and modulating colonic inflammation (17). Its reduction in patients with CAD was consistent with previous findings and underscores its protective role in cardiovascular health (18). Furthermore, the depletion of *Catenibacterium* spp. and *Holdemanella* spp., which are both linked to anti-inflammatory and metabolic benefits (19), suggests that the loss of SCFA-producing bacteria may contribute to metabolic dysregulation and systemic inflammation in CAD. These findings highlight the gut–heart axis and therapeutic potential of restoring SCFA-producing bacteria in CAD management.

Additionally, *S. isoflavoniconvertens*, a bacterium that converts dietary isoflavones into equol, is significantly reduced in patients with CAD. Equol has been linked to anti-inflammatory and cardioprotective properties, and its depletion may contribute to impaired cardiometabolic homeostasis (20). Similar reductions in *S. isoflavoniconvertens* have been reported in lean non-alcoholic fatty liver disease, further supporting its potential role in metabolic disorders (21). *P. copri* (recently renamed *Segatella copri*), a member of the Prevotellaceae family (formerly classified in Bacteroidaceae family), was significantly reduced in patients with CAD. These findings were consistent with other studies reporting the depletion of *Prevotella* and *Bacteroides* species in patients with atherosclerotic CVD (22). The depleted *P. copri* has also been reported to be associated with favorable cardiometabolic profiles, such as lower visceral fat, higher polyunsaturated fatty acids, and reduced C-peptide (23). Notably, *P. vulgatus*, a member of *Bacteroidaceae*, has been associated with protection against atherosclerosis by reducing microbial LPS levels and maintaining barrier function (24), although no significant reduction of *Phocaeicola* species in CAD patients was identified in this study. *Bacteroidaceae* contribute to gut barrier integrity by stimulating mucus production and supporting intestinal epithelial function (25). Disruption of this barrier may allow microbial components such as peptidoglycan and flagellin to translocate into the circulation, promoting systemic inflammation and atherosclerosis (26). These results imply that microbiome-regulated gut barrier health may be a key pathophysiological mechanism in CVD.

Gut microbial metabolic pathways provide critical insights into the pathogenesis of CAD. In this study, we observed a significant enrichment of the urea cycle and L-citrulline biosynthesis in patients with CAD. The urea cycle, which is involved in ammonia detoxification, is linked to CVD severity and mortality via mechanisms related to inflammation and myocardial energetics (27–29). The L-citrulline biosynthesis pathway, primarily driven by *Alistipes* spp., was enriched in CAD cases. Although L-citrulline supplementation has shown blood pressure-lowering effects, recent evidence suggests that it may increase blood pressure during exercise, indicating context-dependent effects (30, 31). Conversely, the depletion of L-isoleucine biosynthesis and BCAA super pathways, which are crucial for muscle nitrogen balance and energy metabolism (32), in CAD cases is consistent with previous findings (33), further supporting its potential contribution to metabolic stress and CAD progression.

The glycolysis III pathway, primarily driven by Enterobacteriaceae family members, such as *E. coli, K. pneumoniae,* and *B. fragilis*, was enriched in CAD cases. As opportunistic

Downloaded from https://journals.asm.org/journal/msystems on 27 May 2026 by 203.255.190.49.

pathogenic bacteria, Enterobacteriaceae may utilize glycolysis to produce inflammatory mediators, such as enterotoxins, promoting systemic inflammation, vascular dysfunction, and the progression of CVD (22). In addition, CDP-diacylglycerol synthesis, a precursor for key phospholipids, such as phosphatidylglycerol and cardiolipin (34), was also enriched in CAD. Bacterial cardiolipin has been linked to inflammation and cell death via Toll-like receptor signaling during host metabolism (35). Interestingly, while these pathways were elevated in our CAD cohort, a previous study reported their depletion in CAD patients (36). These contrasting results suggest that additional factors, such as microbial gene expression, host metabolism, and environmental factors, may play crucial roles in microbial functional shifts in CVD, underscoring the need for cross-cohort validation.

Regarding human gut metabolic functions, CAD cases showed a greater potential for degrading amino acids, particularly arginine and aspartate. This aligns with previous findings showing the enrichment of arginine and serine degradation pathways in patients with CVD, largely driven by pathogenic microbiota (37). The increased microbial conversion of arginine to ornithine and urea may impair NO bioavailability, potentially impairing vascular function and increasing CVD risk (38); in addition to amino acid degradation, patients also have a higher capacity for simple carbohydrate degradation, particularly lactose and xylose. Enrichment of xylose, galactose, and lactose degradation pathways has been associated with an increased production of pro-inflammatory metabolites in patients with CVD and diabetic CAD (39, 40). Collectively, excessive amino acid degradation and the fermentation of simple carbohydrates may exacerbate intestinal barrier dysfunction and contribute to cardiovascular deterioration.

We identified three differentially abundant predicted gut metabolites in patients with CAD. The inosine levels were significantly elevated, which is consistent with previous studies linking inosine to CAD and acute myocardial infarction (41). As a coronary vasodilator, inosine plays a role in relaxing the coronary arteries; however, its precise mechanism remains unclear. Inosine has been implicated in the development of targeted therapeutics for CVDs, cancer, inflammation, and neurological conditions (42). However, its potential role in CVD therapeutics and inflammatory modulation warrants further investigation. C18:0e MAG, a monoacylglycerol phospholipid, is depleted in patients with CAD; however, its role in cardiovascular health remains unknown. Although alpha-muricholic acid was also depleted, its function in the human gut microbiome and its association with CAD require further study.

Random forest classification model analysis highlights the predictive relevance of the gut microbiota and their metabolic products in CAD. Notably, combining differentially abundant bacterial species with predicted microbial metabolites improved the classification performance (area under the curve [AUC] = 0.89) compared with that of models based on either feature alone. This suggests that taxonomic and metabolic information provide complementary insights into the host–microbiome interactions underlying CAD. Among the top predictors, *AM51-8 sp003478275* and *F. prausnitzii* have been previously implicated in metabolic dysregulation and systemic inflammation in CAD (17), whereas metabolites, such as inosine, have been associated with coronary vasodilation (41). These findings support the growing evidence that integrated microbiome features can serve as robust biomarkers for CAD and underscore the potential of multi-omics approaches for microbiome-based diagnostics in CVD.

Using metagenomic assembly and binning, CAD-derived MAGs showed elevated MW-scores for N_2 fixation and sulfite reduction pathways. Enrichment of N_2 fixation could indicate a shift toward microbial self-sufficiency in nitrogen acquisition, potentially compensating for disrupted nitrogen metabolism in the host gut environment (43). Likewise, increased sulfite reduction might be linked to altered sulfur metabolism and increased production of hydrogen sulfide, a gasotransmitter implicated in cardiovascular dysfunction and mucosal inflammation (44). Conversely, control-derived MAGs were enriched in iron reduction, aromatic compound degradation, and nitrite ammonification. Enhanced aromatic degradation may suggest a gut microbiota more equipped for processing complex dietary polyphenols and aromatic compounds, which have been

Downloaded from https://journals.asm.org/journal/msystems on 27 May 2026 by 203.255.190.49.

Downloaded from https://journals.asm.org/journal/msystems on 27 May 2026 by 203.255.190.49.

associated with cardioprotective effects (45). Furthermore, increased iron reduction and nitrite ammonification may reflect a redox-balanced and metabolically versatile microbial community that favors stability over inflammatory triggers (46, 47). These findings suggest that metabolic restructuring of the gut microbiome may play a key role in the ecological adaptation of microbes to host cardiovascular health status.

Interestingly, our strain-level comparative genomic analysis revealed distinct functional profiles between the CAD-derived and control-derived MAGs. Both *M. fumiformis* and *A. muciniphila* have been reported as potentially protective taxa in CVD pathophysiology (48, 49). However, the CAD-derived *M. fumiformis* strain showed carriage of functional modules for acetate-centered metabolism (methanogenesis/methanotroph, SCFA conversion), mercury reduction, and fatty acid degradation, indicating a shift toward pro-atherogenic metabolism (50, 51), compared with those in control-derived MAGs. Additionally, *A. muciniphila* MAGs from controls carried more functional modules for complex carbohydrate degradation (e.g., arabinan, xyloglucan), potentially mucosal protective and anti-inflammatory properties (48). However, given that these interferences from gene presence/absence, not capturing expression, regulation, enzyme activity, or physiological context, further experimental validation seems to be needed to prove their biological relevance. These findings underscore the critical importance of strain-level functional heterogeneity, as revealed through MAG-based analysis, in shaping host–microbe interactions and influencing CAD pathophysiology.

Despite the well-established link between TMAO and CVD (52), our study found no significant differences in TMAO-related gene abundances between CAD and control groups when mapping individual fastq samples to the TMA-related gene database. Consistently, Griffin et al. highlighted that choline oxidation and TMAO production were not predictive of atherosclerotic plaque formation in animal models. (53, 54). However, genome-resolved MAGs analysis in the present study has provided deeper insights into the strain-specific distribution of TMA-related genes. Notably, the *cutC* gene (55), responsible for choline-to-TMA conversion, was detected in *A. hadrus* MAGs from both CAD and control groups, whereas the *cntA/yeaW* gene (56, 57), associated with TMA production from ammonium compounds like carnitine and γ-butyrobetaine, was present in *M. fumiformis* MAGs from both CAD and control groups. Although both *A. hadrus* and *M. fumiformis* are generally regarded as SCFA producers (49, 58), our MAG-based analysis revealed carriage of TMA-producing genes in their genomes, suggesting a potential dual role in gut-host interactions. On the other hand, among the reported non-TMA-producing genes, *mtxB* (quaternary amine methyltransferase) (59) was detected in *P. plebeius_A* and *F. prausnitzii* species MAGs from only the control group, while *mttB* (trimethylamine methyltransferase) (60) was detected in *Phocaeicola* species MAGs from both CAD and control groups. *Phocaeicola* species and *F. prausnitzii* are well recognized for their anti-inflammatory traits (17). Given that *F. prausnitzii* was significantly depleted in CAD cases in our MetaPhlAn4-based differential abundance analysis, this observation suggests that *F. prausnitzii* could play a potential protective role in CAD pathophysiology. Together, these findings highlight the value of MAG-based approaches for uncovering strain-level functional heterogeneity that may be obscured in community-level analyses. Therefore, it is important to elucidate the microbial contributions to TMAO metabolism and their subtle roles in CAD pathogenesis.

Despite these novel findings, this study had some limitations. First, the relatively small and sex-imbalanced sample size may limit the robustness and generalizability of the findings despite the use of PSM to reduce confounding factors. Second, the cross-sectional design precludes causal inference, highlighting the need for longitudinal studies to clarify microbial dynamics in CAD progression. Third, while shotgun metagenomics enables strain-level resolution and provides valuable insights into the metabolic potential of microbial communities, it has limited capacity to capture the *in situ* activity of these pathways. Future studies integrating metatranscriptomics, metaproteomics, or metabolomics will be needed to directly assess functional activity and host-microbe interactions. Despite these limitations, this is the first study to report the discovery of

distinctive bacterial MAGs in patients with CAD and healthy controls, offering novel insights into the role of the gut microbiome in the pathophysiology of CAD.

In conclusion, this study provides a comprehensive characterization of the gut microbial signature associated with CAD using shotgun metagenomics. These findings underscore the importance of gut microbial and functional profiling in understanding CAD and provide a foundation for microbiome-targeted therapeutic strategies for CAD management and risk reduction. Future studies should focus on validating these microbial signatures in larger cohorts and exploring their mechanistic roles in cardiovascular health.

MATERIALS AND METHODS

Study subjects, data collection, and group definition

This cross-sectional study was part of the Kangbuk Samsung Cohort Study involving 1,710 Korean adults (aged 23–77 years) who underwent regular health screening between 2014 and 2021 (61). Medical histories, medication use, and lifestyle factors were assessed using structured questionnaires. Anthropometrics, blood pressure, and blood samples were analyzed using standardized protocols. The methodological details of data collection are provided in the Supplemental Methods. After excluding individuals based on recent antibiotic use, antacid use, history of cancer, or history of stroke, 1,585 participants remained (Fig. S1A).

CAD was diagnosed in individuals with a documented history of angina pectoris, myocardial ischemia, or angiographically confirmed stenosis (>50%) in at least one major coronary artery (33). To minimize the imbalance between patients with CAD and controls, PSM was performed using age, sex, and BMI as covariates. In total, 42 participants (14 CAD cases and 28 controls) were included in the final matched analysis (Fig. S1B). The methodological details of PSM are provided in the Supplemental Methods.

DNA extraction and shotgun metagenomic sequencing

Detailed methods for fecal sample collection, metagenomic DNA extraction, shotgun metagenomic sequencing, and raw metagenomic data pre-processing are provided in the Supplemental Methods.

Taxonomic and functional profiling of metagenomic data

For taxonomic classification, metagenomic reads were analyzed using MetaPhlAn4 (v.4.0.6) (62) with default parameters. Only the microbial species present in at least 10% of the samples were included in the analysis to mitigate the impact of rare taxa (63). Functional profiling was performed using HUMAnN3 (v.3.0) (64). To visualize species-level contributions to metabolic pathways, stratified relative abundance bar plots were generated using the humann_bar plot function in HUMAnN3 (64). MelonnPan was used to predict microbial metabolites with the UniRef90 gene profile as the input data (65). Functional genes associated with human gut metabolites were analyzed using the curated GMM database (13) using Omixer-RPM (v0.3.2) (66), with a 33.3% minimum coverage threshold. Taxonomic profiles, functional genes, and GMM modules were all calculated as relative abundances. TMA-related genes were quantified based on reads per kilobase per million mapped reads (RPKM) with the Methylated Amine Gene Inventory of Catabolism database (MAGICdb) (67) using CoverM (v.0.7.0) (68).

MAG reconstruction and phylogenetic analysis

To reconstruct MAGs, we performed both co-assemblies for the CAD and control groups and individual assemblies for all samples. All high-quality non-human reads were pooled for each group and assembled independently using MEGAHIT (v.1.2.9) (69), excluding contigs shorter than 1 kb. Binning of the assembled contigs was performed using three

Downloaded from https://journals.asm.org/journal/msystems on 27 May 2026 by 203.255.190.49.

independent binning algorithms: MaxBin2 (70), MetaBAT2 (71), and CONCOCT (72). The resulting bins were refined using DAStool (73) to obtain near-complete genomes with minimal contamination. Genome quality was assessed using CheckM (74), applying strict thresholds of >90% completeness and <10% contamination for the final bin selection (Tables S4 and S7). The taxonomic classification of MAGs was determined using GTDB-tk (v2.0) (75) from the GTDB database (v.214). Dereplication of individual MAGs was performed at thresholds of 95% ANI with dRep (v.3.4.2) (76). Relative abundances of both co-assembly MAGs and dereplicated individual MAGs across samples were quantified using CoverM (v.0.7.0).

To assess potential metabolic interactions within microbial communities, we utilized METABOLIC (v4.0) (14) for community-scale metabolic profiling of MAGs using MW-scores, representing the relative contribution of each function to the total community capacity. The species-level contributions to each metabolic pathway were calculated using the METABOLIC-C.pl function in METABOLIC (14). Furthermore, to investigate the genome-wide functional potential, we annotated MAGs based on DRAM-implemented functional modules (15), lipids (KEGG: 09103), CVD (KEGG:09166)-associated KEGG orthologs (77), and MAGICdb-implemented TMA-related genes (67). Phylogenetic trees were constructed using PhyloPhlAn (v.3.0) (78). The iTol web server (v.7, https://itol.embl.de/) (79) was used to visualize the functional analysis of MAGs.

To evaluate the metabolic features and genetic diversity of MAGs identified in this study against reference genomes, we conducted strain-level comparative genomic analysis for four species (*B. aalborgi*, *M. fumiformis*, *A. muciniphila*, and *S. wadsworthensis*), identified in both case and control MAGs as well as individual MAGs, using a public database, the Bacterial and Viral Bioinformatics Resource Center (BV-BRC) (80). Whole genome sequences of human-derived bacterial species with available metadata (e.g., country of origin and year of isolation) were utilized, totaling 34 *B. aalborgi*, 53 *M. fumiformis*, 204 *S. wadsworthensis*, and 429 *A. muciniphila* strains (accessed on 25 May 25 2025; Table S10). Comparative genomic analyses were conducted using the same pipeline as that used for MAGs identified in this study.

Statistical analysis

Alpha and beta diversity indices were computed to assess microbial community structure using the vegan R package (v.2.6.4) (81). Alpha diversity (Chao, Simpson, Shannon, and Pielou's evenness) was calculated, and group differences were assessed using the Wilcoxon rank-sum test. Beta diversity was computed based on Bray–Curtis dissimilarity, and intergroup significance was tested using PERMANOVA with 999 permutations.

To identify group differences in microbial taxa, MetaCyc metabolic pathways, GMMs, and predicted metabolites, we applied generalized linear models using the Microbiome Multivariable Association with Linear Models 2 (MaAsLin2) (82). In the MaAsLin2 models, we estimated the coefficients of log-transformed relative abundance by comparing the CAD group with the reference control group. Differential abundance of TMA-related genes was assessed using the Wilcoxon rank-sum test.

To assess the predictive potential of microbial features in distinguishing patients with CAD from controls, we applied a random forest classification model using three feature sets: the differential abundances of (i) bacterial species (ii), predicted microbial metabolites, and (iii) both bacterial species and metabolites. The model performance was evaluated using fivefold cross-validation (500 decision trees per model, 50 iterations). The ROC curves and AUC values were computed across iterations. The feature importance was determined using the mean decrease Gini index. The results are summarized as mean values across iterations with 95% CIs. Predictive model analyses were performed using Python (v3.10.18) with Pandas (v2.3.0), sklearn (v1.7.0), and matplotlib (v3.10.3).

Downloaded from https://journals.asm.org/journal/msystems on 27 May 2026 by 203.255.190.49.

ACKNOWLEDGMENTS

This work was supported by a National Research Foundation of Korea (NRF) grant funded by the Korean Government (MSIT) (no. RS-2023-NR077149).

AUTHOR AFFILIATIONS

[1]Department of Clinical Research Design and Evaluation, Samsung Advanced Institute for Health Sciences & Technology, Sungkyunkwan University, Seoul, Republic of Korea
[2]Center for Cohort Studies, Total Healthcare Center, Kangbuk Samsung Hospital, Sungkyunkwan University School of Medicine, Seoul, Republic of Korea
[3]Department of Occupational and Environmental Medicine, Kangbuk Samsung Hospital, Sungkyunkwan University School of Medicine, Seoul, Republic of Korea
[4]Department of Biochemistry, College of Medicine, Ewha Womans University, Seoul, Republic of Korea
[5]Cardiovascular Center, Seoul National University Bundang Hospital, Seongnam-si, Republic of Korea
[6]Department of Internal Medicine, Seoul National University, Seoul, Republic of Korea
[7]Center for Clinical Epidemiology, Samsung Medical Center, Sungkyunkwan University, Seoul, Republic of Korea

AUTHOR ORCIDs

Seungho Ryu https://orcid.org/0000-0002-3927-8646
Han-Na Kim http://orcid.org/0000-0001-7053-7469

FUNDING

Funder	Grant(s)	Author(s)
National Research Foundation of Korea	RS-2023-NR077149	Han-Na Kim

AUTHOR CONTRIBUTIONS

Soomin Lee, Formal analysis, Methodology, Validation, Visualization, Writing – original draft, Writing – review and editing | Shahbaz Raza, Formal analysis, Methodology, Software | Eun-Ju Lee, Formal analysis, Methodology, Software | Yoosoo Chang, Data curation, Investigation, Writing – review and editing | Seungho Ryu, Data curation, Investigation, Writing – review and editing | Hyung-Lae Kim, Data curation, Investigation, Resources, Writing – review and editing | Si-Hyuck Kang, Investigation, Writing – review and editing | Han-Na Kim, Conceptualization, Data curation, Formal analysis, Funding acquisition, Supervision, Writing – original draft, Writing – review and editing

DATA AVAILABILITY

Raw sequencing data generated in this study have been deposited in the NCBI Sequence Read Archive under accession number PRJNA1195215. Analysis codes, intermediate files, and STORM checklists are publicly available at Zenodo (https://doi.org/10.5281/zenodo.17250068) and are also provided in the Supplemental Material.

ETHICS APPROVAL

This study was approved by the Institutional Review Board of Sungkyunkwan University (SKKU 2023-11-034), and written informed consent was obtained from all participants. The current study was conducted under the Declaration of Helsinki.

ADDITIONAL FILES

The following material is available online.

Downloaded from https://journals.asm.org/journal/msystems on 27 May 2026 by 203.255.190.49.

Supplemental Material

Supplemental Material (mSystems00954-25-S0001.pdf). Supplemental methods; Fig. S1 to S11.
Supplemental Tables (mSystems00954-25-S0002.xlsx). Tables S1 to S10.

REFERENCES

1. Martin SS, Aday AW, Almarzooq ZI, Anderson CAM, Arora P, Avery CL, Baker-Smith CM, Barone Gibbs B, Beaton AZ, Boehme AK, et al. 2024. 2024 heart disease and stroke statistics: a report of US and global data from the American Heart Association. Circulation 149:e347–e913. https://doi.org/10.1161/CIR.0000000000001209
2. Jin DL, Kim KH, Chung ES, Yoon SJ. 2024. Trends in regional disparities in cardiovascular surgery and mortality in Korea: a national cross-sectional study. J Prev Med Public Health 57:260–268. https://doi.org/10.3961/jpmph.24.057
3. Zhu W, Gregory JC, Org E, Buffa JA, Gupta N, Wang Z, Li L, Fu X, Wu Y, Mehrabian M, Sartor RB, McIntyre TM, Silverstein RL, Tang WHW, DiDonato JA, Brown JM, Lusis AJ, Hazen SL. 2016. Gut microbial metabolite TMAO enhances platelet hyperreactivity and thrombosis risk. Cell 165:111–124. https://doi.org/10.1016/j.cell.2016.02.011
4. Koeth RA, Wang Z, Levison BS, Buffa JA, Org E, Sheehy BT, Britt EB, Fu X, Wu Y, Li L, Smith JD, DiDonato JA, Chen J, Li H, Wu GD, Lewis JD, Warrier M, Brown JM, Krauss RM, Tang WHW, Bushman FD, Lusis AJ, Hazen SL. 2013. Intestinal microbiota metabolism of L-carnitine, a nutrient in red meat, promotes atherosclerosis. Nat Med 19:576–585. https://doi.org/10.1038/nm.3145
5. Qi J, You T, Li J, Pan T, Xiang L, Han Y, Zhu L. 2018. Circulating trimethylamine N-oxide and the risk of cardiovascular diseases: a systematic review and meta-analysis of 11 prospective cohort studies. J Cell Mol Med 22:185–194. https://doi.org/10.1111/jcmm.13307
6. Kazemian N, Mahmoudi M, Halperin F, Wu JC, Pakpour S. 2020. Gut microbiota and cardiovascular disease: opportunities and challenges. Microbiome 8:36. https://doi.org/10.1186/s40168-020-00821-0
7. Moludi J, Kafil HS, Qaisar SA, Gholizadeh P, Alizadeh M, Vayghyan HJ. 2021. Effect of probiotic supplementation along with calorie restriction on metabolic endotoxemia, and inflammation markers in coronary artery disease patients: a double blind placebo controlled randomized clinical trial. Nutr J 20:47. https://doi.org/10.1186/s12937-021-00703-7
8. Suresh MG, Mohamed S, Yukselen Z, Hatwal J, Venkatakrishnan A, Metri A, Bhardwaj A, Singh A, Bush N, Batta A. 2025. Therapeutic modulation of gut microbiome in cardiovascular disease: a literature review. Heart Mind 9:68–79. https://doi.org/10.4103/hm.HM-D-24-00044
9. Wensel CR, Pluznick JL, Salzberg SL, Sears CL. 2022. Next-generation sequencing: insights to advance clinical investigations of the microbiome. J Clin Invest 132:e154944. https://doi.org/10.1172/JCI154944
10. Jovel J, Patterson J, Wang W, Hotte N, O'Keefe S, Mitchel T, Perry T, Kao D, Mason AL, Madsen KL, Wong GK-S. 2016. Characterization of the gut microbiome using 16s or shotgun metagenomics. Front Microbiol 7:459. https://doi.org/10.3389/fmicb.2016.00459
11. Zeng S, Patangia D, Almeida A, Zhou Z, Mu D, Paul Ross R, Stanton C, Wang S. 2022. A compendium of 32,277 metagenome-assembled genomes and over 80 million genes from the early-life human gut microbiome. Nat Commun 13:5139. https://doi.org/10.1038/s41467-022-32805-z
12. Franzosa EA, McIver LJ, Rahnavard G, Thompson LR, Schirmer M, Weingart G, Lipson KS, Knight R, Caporaso JG, Segata N, Huttenhower C. 2018. Species-level functional profiling of metagenomes and metatranscriptomes. Nat Methods 15:962–968. https://doi.org/10.1038/s41592-018-0176-y
13. Vieira-Silva S, Falony G, Darzi Y, Lima-Mendez G, Garcia Yunta R, Okuda S, Vandeputte D, Valles-Colomer M, Hildebrand F, Chaffron S, Raes J. 2016. Species-function relationships shape ecological properties of the human gut microbiome. Nat Microbiol 1:16088. https://doi.org/10.1038/nmicrobiol.2016.88
14. Zhou Z, Tran PQ, Breister AM, Liu Y, Kieft K, Cowley ES, Karaoz U, Anantharaman K. 2022. METABOLIC: high-throughput profiling of microbial genomes for functional traits, metabolism, biogeochemistry, and community-scale functional networks. Microbiome 10:33. https://doi.org/10.1186/s40168-021-01213-8
15. Shaffer M, Borton MA, McGivern BB, Zayed AA, La Rosa SL, Solden LM, Liu P, Narrowe AB, Rodríguez-Ramos J, Bolduc B, Gazitúa MC, Daly RA, Smith GJ, Vik DR, Pope PB, Sullivan MB, Roux S, Wrighton KC. 2020. DRAM for distilling microbial metabolism to automate the curation of microbiome function. Nucleic Acids Res 48:8883–8900. https://doi.org/10.1093/nar/gkaa621
16. Choroszy M, Litwinowicz K, Bednarz R, Roleder T, Lerman A, Toya T, Kamiński K, Sawicka-Śmiarowska E, Niemira M, Sobieszczańska B. 2022. Human gut microbiota in coronary artery disease: a systematic review and meta-analysis. Metabolites 12:1165. https://doi.org/10.3390/metabo12121165
17. Gomaa EZ. 2020. Human gut microbiota/microbiome in health and diseases: a review. Antonie Van Leeuwenhoek 113:2019–2040. https://doi.org/10.1007/s10482-020-01474-7
18. Trøseid M, Andersen GØ, Broch K, Hov JR. 2020. The gut microbiome in coronary artery disease and heart failure: current knowledge and future directions. EBioMedicine 52:102649. https://doi.org/10.1016/j.ebiom.2020.102649
19. Ma Y, Zhu L, Ma Z, Gao Z, Wei Y, Shen Y, Li L, Liu X, Ren M. 2021. Distinguishing feature of gut microbiota in Tibetan highland coronary artery disease patients and its link with diet. Sci Rep 11:18486. https://doi.org/10.1038/s41598-021-98075-9
20. Setchell KDR, Clerici C, Lephart ED, Cole SJ, Heenan C, Castellani D, Wolfe BE, Nechemias-Zimmer L, Brown NM, Lund TD, Handa RJ, Heubi JE. 2005. S-equol, a potent ligand for estrogen receptor beta, is the exclusive enantiomeric form of the soy isoflavone metabolite produced by human intestinal bacterial flora. Am J Clin Nutr 81:1072–1079. https://doi.org/10.1093/ajcn/81.5.1072
21. Iino C, Endo T, Iino K, Tateda T, Sato S, Igarashi G, Mikami K, Sakuraba H, Yokoyama Y, Nakaji S, Fukuda S. 2022. Reduced equol production and gut microbiota features in men with lean nonalcoholic fatty liver disease. Am J Mens Health 16:15579883221115598. https://doi.org/10.1177/15579883221115598
22. Jie Z, Xia H, Zhong S-L, Feng Q, Li S, Liang S, Zhong H, Liu Z, Gao Y, Zhao H, et al. 2017. The gut microbiome in atherosclerotic cardiovascular disease. Nat Commun 8:845. https://doi.org/10.1038/s41467-017-00900-1
23. Abdelsalam NA, Hegazy SM, Aziz RK. 2023. The curious case of *Prevotella copri*. Gut Microbes 15:2249152. https://doi.org/10.1080/19490976.2023.2249152
24. Yoshida N, Emoto T, Yamashita T, Watanabe H, Hayashi T, Tabata T, Hoshi N, Hatano N, Ozawa G, Sasaki N, Mizoguchi T, Amin HZ, Hirota Y, Ogawa W, Yamada T, Hirata K-I. 2018. *Bacteroides vulgatus* and *Bacteroides dorei* reduce gut microbial lipopolysaccharide production and inhibit atherosclerosis. Circulation 138:2486–2498. https://doi.org/10.1161/CIRCULATIONAHA.118.033714
25. Kelly CJ, Zheng L, Campbell EL, Saeedi B, Scholz CC, Bayless AJ, Wilson KE, Glover LE, Kominsky DJ, Magnuson A, Weir TL, Ehrentraut SF, Pickel C, Kuhn KA, Lanis JM, Nguyen V, Taylor CT, Colgan SP. 2015. Crosstalk between microbiota-derived short-chain fatty acids and intestinal epithelial HIF augments tissue barrier function. Cell Host Microbe 17:662–671. https://doi.org/10.1016/j.chom.2015.03.005
26. Escalante J, Artaiz O, Diwakarla S, McQuade RM. 2025. Leaky gut in systemic inflammation: exploring the link between gastrointestinal disorders and age-related diseases. Geroscience 47:1–22. https://doi.org/10.1007/s11357-024-01451-2
27. Prechtl L, Carrard J, Gallart-Ayala H, Borreggine R, Teav T, Königstein K, Wagner J, Knaier R, Infanger D, Streese L, Hinrichs T, Hanssen H, Ivanisevic J, Schmidt-Trucksäss A. 2024. Circulating amino acid signature features urea cycle alterations associated with coronary artery disease. Sci Rep 14:25848. https://doi.org/10.1038/s41598-024-76835-7
28. Pernow J, Jung C. 2013. Arginase as a potential target in the treatment of cardiovascular disease: reversal of arginine steal? Cardiovasc Res 98:334–343. https://doi.org/10.1093/cvr/cvt036
29. Mehta A, Liu C, Nayak A, Tahhan AS, Ko Y-A, Dhindsa DS, Kim JH, Hayek SS, Sperling LS, Mehta PK, Sun YV, Uppal K, Jones DP, Quyyumi AA. 2020. Untargeted high-resolution plasma metabolomic profiling predicts

Downloaded from https://journals.asm.org/journal/msystems on 27 May 2026 by 203.255.190.49.

Downloaded from https://journals.asm.org/journal/msystems on 27 May 2026 by 203.255.190.49.

outcomes in patients with coronary artery disease. PLoS One 15:e0237579. https://doi.org/10.1371/journal.pone.0237579
30. Barkhidarian B, Khorshidi M, Shab-Bidar S, Hashemi B. 2019. Effects of L-citrulline supplementation on blood pressure: a systematic review and meta-analysis. Avicenna J Phytomed 9:10–20. https://doi.org/10.22038/ajp.2018.11590
31. Tryfonos A, Christodoulou F, Pamboris GM, Christodoulides S, Theodorou AA. 2023. Short-term L-citrulline supplementation does not affect blood pressure, pulse wave reflection, or arterial stiffness at rest and during isometric exercise in older males. Sports 11:177. https://doi.org/10.3390/sports11090177
32. Zheng L, Mingxue Z, Zeng L, Yushi Z, Yuhan A, Yi Y, Botong L. 2022. A landscape of metabonomics for intermingled phlegm and blood stasis and its concurrent syndromes in stable angina pectoris of coronary heart disease. Front Cardiovasc Med 9:871142. https://doi.org/10.3389/fcvm.2022.871142
33. Zhong J, Wu D, Zeng Y, Wu G, Zheng N, Huang W, Li Y, Tao X, Zhu W, Sheng L, Shen X, Zhang W, Zhu R, Li H. 2022. The microbial and metabolic signatures of patients with stable coronary artery disease. Microbiol Spectr 10:e02467-22. https://doi.org/10.1128/spectrum.02467-22
34. Parsons JB, Rock CO. 2013. Bacterial lipids: metabolism and membrane homeostasis. Prog Lipid Res 52:249–276. https://doi.org/10.1016/j.plipres.2013.02.002
35. Tiku V, Kew C, Kofoed EM, Peng Y, Dikic I, Tan MW. 2022. *Acinetobacter baumannii* secretes a bioactive lipid that triggers inflammatory signaling and cell death. Front Microbiol 13:870101. https://doi.org/10.3389/fmicb.2022.870101
36. Liu S, Zhao W, Liu X, Cheng L. 2020. Metagenomic analysis of the gut microbiome in atherosclerosis patients identify cross - cohort microbial signatures and potential therapeutic target. The FASEB Journal 34:14166–14181. https://doi.org/10.1096/fj.202000622R
37. Li T-T, Chen X, Huo D, Arifuzzaman M, Qiao S, Jin W-B, Shi H, Li XV, Iliev ID, Artis D, Guo C-J. 2024. Microbiota metabolism of intestinal amino acids impacts host nutrient homeostasis and physiology. Cell Host Microbe 32:661–675. https://doi.org/10.1016/j.chom.2024.04.004
38. Durante W, Johnson FK, Johnson RA. 2007. Arginase: a critical regulator of nitric oxide synthesis and vascular function. Clin Exp Pharmacol Physiol 34:906–911. https://doi.org/10.1111/j.1440-1681.2007.04638.x
39. Li Y, Liu Y, Cui J, Zhu M, Wang W, Chen K, Huang L, Liu Y. 2024. Oral-gut microbial transmission promotes diabetic coronary heart disease. Cardiovasc Diabetol 23:123. https://doi.org/10.1186/s12933-024-02217-y
40. Hu X, Zhou R, Li H, Zhao X, Sun Y, Fan Y, Zhang S. 2021. Alterations of gut microbiome and serum metabolome in coronary artery disease patients complicated with non-alcoholic fatty liver disease are associated with adverse cardiovascular outcomes. Front Cardiovasc Med 8:805812. https://doi.org/10.3389/fcvm.2021.805812
41. Farthing DE, Farthing CA, Xi L. 2015. Inosine and hypoxanthine as novel biomarkers for cardiac ischemia: from bench to point-of-care. Exp Biol Med (Maywood) 240:821–831. https://doi.org/10.1177/1535370215584931
42. Kim IS, Jo E-K. 2022. Inosine: a bioactive metabolite with multimodal actions in human diseases. Front Pharmacol 13:1043970. https://doi.org/10.3389/fphar.2022.1043970
43. Igai K, Itakura M, Nishijima S, Tsurumaru H, Suda W, Tsutaya T, Tomitsuka E, Tadokoro K, Baba J, Odani S, Natsuhara K, Morita A, Yoneda M, Greenhill AR, Horwood PF, Inoue J-I, Ohkuma M, Hongoh Y, Yamamoto T, Siba PM, Hattori M, Minamisawa K, Umezaki M. 2016. Nitrogen fixation and nifH diversity in human gut microbiota. Sci Rep 6:31942. https://doi.org/10.1038/srep31942
44. Pan LL, Qin M, Liu XH, Zhu YZ. 2017. The role of hydrogen sulfide on cardiovascular homeostasis: an overview with update on immunomodulation. Front Pharmacol 8:686. https://doi.org/10.3389/fphar.2017.00686
45. Cano R, Bermúdez V, Galban N, Garrido B, Santeliz R, Gotera MP, Duran P, Boscan A, Carbonell-Zabaleta A-K, Durán-Agüero S, Rojas-Gómez D, González-Casanova J, Díaz-Vásquez W, Chacín M, Angarita Dávila L. 2024. Dietary polyphenols and gut microbiota cross-talk: molecular and therapeutic perspectives for cardiometabolic disease: a narrative review. Int J Mol Sci 25:9118. https://doi.org/10.3390/ijms25169118
46. Coby AJ, Picardal F, Shelobolina E, Xu H, Roden EE. 2011. Repeated anaerobic microbial redox cycling of iron. Appl Environ Microbiol 77:6036–6042. https://doi.org/10.1128/AEM.00276-11
47. Rocha BS, Laranjinha J. 2020. Nitrate from diet might fuel gut microbiota metabolism: minding the gap between redox signaling and inter-kingdom communication. Free Radic Biol Med 149:37–43. https://doi.org/10.1016/j.freeradbiomed.2020.02.001
48. Gofron K, Berezowski A, Gofron M, Borówka M, Dziedzic M, Kazimierczak W, Kwiatkowski M, Gofron M, Nowaczyk Z, Małgorzewicz S. 2024. *Akkermansia muciniphila* - impact on the cardiovascular risk, the intestine inflammation and obesity. Acta Biochim Pol 71:13550. https://doi.org/10.3389/abp.2024.13550
49. Yang X, Zhang M, Liu Y, Wei F, Li X, Feng Y, Jin X, Liu D, Guo Y, Hu Y. 2023. Inulin-enriched Megamonas funiformis ameliorates metabolic dysfunction-associated fatty liver disease by producing propionic acid. NPJ Biofilms Microbiomes 9:84. https://doi.org/10.1038/s41522-023-00451-y
50. Volmer JG, McRae H, Morrison M. 2023. The evolving role of methanogenic archaea in mammalian microbiomes. Front Microbiol 14:1268451. https://doi.org/10.3389/fmicb.2023.1268451
51. Rogero MM, Calder PC. 2018. Obesity, inflammation, toll-like receptor 4 and fatty acids. Nutrients 10:432. https://doi.org/10.3390/nu10040432
52. Tang WHW, Wang Z, Levison BS, Koeth RA, Britt EB, Fu X, Wu Y, Hazen SL. 2013. Intestinal microbial metabolism of phosphatidylcholine and cardiovascular risk. N Engl J Med 368:1575–1584. https://doi.org/10.1056/NEJMoa1109400
53. Ferrell M, Bazeley P, Wang Z, Levison BS, Li XS, Jia X, Krauss RM, Knight R, Lusis AJ, Garcia-Garcia JC, Hazen SL, Tang WHW. 2021. Fecal microbiome composition does not predict diet-induced TMAO production in healthy adults. J Am Heart Assoc 10:e021934. https://doi.org/10.1161/JAHA.121.021934
54. Griffin JL, Wang X, Stanley E. 2015. Does our gut microbiome predict cardiovascular risk? A review of the evidence from metabolomics. Circ Cardiovasc Genet 8:187–191. https://doi.org/10.1161/CIRCGENETICS.114.000219
55. Craciun S, Balskus EP. 2012. Microbial conversion of choline to trimethylamine requires a glycyl radical enzyme. Proc Natl Acad Sci USA 109:21307–21312. https://doi.org/10.1073/pnas.1215689109
56. Koeth RA, Levison BS, Culley MK, Buffa JA, Wang Z, Gregory JC, Org E, Wu Y, Li L, Smith JD, Tang WHW, DiDonato JA, Lusis AJ, Hazen SL. 2014. γ-Butyrobetaine is a proatherogenic intermediate in gut microbial metabolism of L-carnitine to TMAO. Cell Metab 20:799–812. https://doi.org/10.1016/j.cmet.2014.10.006
57. Zhu Y, Jameson E, Crosatti M, Schäfer H, Rajakumar K, Bugg TDH, Chen Y. 2014. Carnitine metabolism to trimethylamine by an unusual Rieske-type oxygenase from human microbiota. Proc Natl Acad Sci USA 111:4268–4273. https://doi.org/10.1073/pnas.1316569111
58. Bui TPN, Mannerås-Holm L, Puschmann R, Wu H, Troise AD, Nijsse B, Boeren S, Bäckhed F, Fiedler D, deVos WM. 2021. Conversion of dietary inositol into propionate and acetate by commensal Anaerostipes associates with host health. Nat Commun 12:4798. https://doi.org/10.1038/s41467-021-25081-w
59. Ticak T, Kountz DJ, Girosky KE, Krzycki JA, Ferguson DJ Jr. 2014. A nonpyrrolysine member of the widely distributed trimethylamine methyltransferase family is a glycine betaine methyltransferase. Proc Natl Acad Sci USA 111:E4668–E4676. https://doi.org/10.1073/pnas.1409642111
60. Ferguson DJ Jr, Krzycki JA. 1997. Reconstitution of trimethylamine-dependent coenzyme M methylation with the trimethylamine corrinoid protein and the isozymes of methyltransferase II from *Methanosarcina barkeri*. J Bacteriol 179:846–852. https://doi.org/10.1128/jb.179.3.846-852.1997
61. Chang Y, Cho YK, Kim Y, Sung E, Ahn J, Jung HS, Yun KE, Shin H, Ryu S. 2019. Nonheavy drinking and worsening of noninvasive fibrosis markers in nonalcoholic fatty liver disease: a cohort study. Hepatology 69:64–75. https://doi.org/10.1002/hep.30170
62. Blanco-Míguez A, Beghini F, Mclver LJ, Thompson KN, Zolfo M, Manghi P, Dubois L, Huang KD, Thomas AM, Nickols WA, Piccinno G, Piperni E, Punčochář M, Valles-Colomer M, Tett A, Giordano F, Davies R, Wolf J, Berry SE, Spector TD, Franzosa EA, Pasolli E, Asnicar F, Huttenhower C, Segata N. 2023. Extending and improving metagenomic taxonomic profiling with uncharacterized species using MetaPhlAn 4. Nat Biotechnol 41:1633-1644. https://doi.org/10.1038/s41587-023-01688-w
63. Zhang Y, Fan Q, Hou Y, Zhang X, Yin Z, Cai X, Wei W, Wang J, He D, Wang G, Yuan Y, Hao H, Zheng X. 2022. Bacteroides species differentially modulate depression-like behavior via gut-brain metabolic signaling.

Brain Behav Immun 102:11–22. https://doi.org/10.1016/j.bbi.2022.02.007
64. Beghini F, McIver LJ, Blanco-Míguez A, Dubois L, Asnicar F, Maharjan S, Mailyan A, Manghi P, Scholz M, Thomas AM, Valles-Colomer M, Weingart G, Zhang Y, Zolfo M, Huttenhower C, Franzosa EA, Segata N. 2021. Integrating taxonomic, functional, and strain-level profiling of diverse microbial communities with bioBakery 3. elife 10:e65088. https://doi.org/10.7554/eLife.65088
65. Mallick H, Franzosa EA, McIver LJ, Banerjee S, Sirota-Madi A, Kostic AD, Clish CB, Vlamakis H, Xavier RJ, Huttenhower C. 2019. Predictive metabolomic profiling of microbial communities using amplicon or metagenomic sequences. Nat Commun 10:3136. https://doi.org/10.1038/s41467-019-10927-1
66. Darzi Y, Falony G, Vieira-Silva S, Raes J. 2016. Towards biome-specific analysis of meta-omics data. ISME J 10:1025–1028. https://doi.org/10.1038/ismej.2015.188
67. Borton MA, Shaffer M, Hoyt DW, Jiang R, Ellenbogen JB, Purvine S, Nicora CD, Eder EK, Wong AR, Smulian AG, Lipton MS, Krzycki JA, Wrighton KC. 2023. Targeted curation of the gut microbial gene content modulating human cardiovascular disease. mBio 14:e01511-23. https://doi.org/10.1128/mbio.01511-23
68. Aroney STN, Newell RJP, Nissen JN, Camargo AP, Tyson GW, Woodcroft BJ. 2025. CoverM: read alignment statistics for metagenomics. Bioinformatics 41:btaf147. https://doi.org/10.1093/bioinformatics/btaf147
69. Li D, Liu C-M, Luo R, Sadakane K, Lam T-W. 2015. MEGAHIT: an ultra-fast single-node solution for large and complex metagenomics assembly via succinct de Bruijn graph. Bioinformatics 31:1674–1676. https://doi.org/10.1093/bioinformatics/btv033
70. Wu Y-W, Simmons BA, Singer SW. 2016. MaxBin 2.0: an automated binning algorithm to recover genomes from multiple metagenomic datasets. Bioinformatics 32:605–607. https://doi.org/10.1093/bioinformatics/btv638
71. Kang DD, Li F, Kirton E, Thomas A, Egan R, An H, Wang Z. 2019. MetaBAT 2: an adaptive binning algorithm for robust and efficient genome reconstruction from metagenome assemblies. PeerJ 7:e7359. https://doi.org/10.7717/peerj.7359
72. Alneberg J, Bjarnason BS, de Bruijn I, Schirmer M, Quick J, Ijaz UZ, Lahti L, Loman NJ, Andersson AF, Quince C. 2014. Binning metagenomic contigs by coverage and composition. Nat Methods 11:1144–1146. https://doi.org/10.1038/nmeth.3103
73. Sieber CMK, Probst AJ, Sharrar A, Thomas BC, Hess M, Tringe SG, Banfield JF. 2018. Recovery of genomes from metagenomes via a dereplication, aggregation and scoring strategy. Nat Microbiol 3:836–843. https://doi.org/10.1038/s41564-018-0171-1
74. Parks DH, Imelfort M, Skennerton CT, Hugenholtz P, Tyson GW. 2015. CheckM: assessing the quality of microbial genomes recovered from isolates, single cells, and metagenomes. Genome Res 25:1043–1055. https://doi.org/10.1101/gr.186072.114
75. Chaumeil P-A, Mussig AJ, Hugenholtz P, Parks DH. 2022. GTDB-Tk v2: memory friendly classification with the genome taxonomy database. Bioinformatics 38:5315–5316. https://doi.org/10.1093/bioinformatics/btac672
76. Olm MR, Brown CT, Brooks B, Banfield JF. 2017. dRep: a tool for fast and accurate genomic comparisons that enables improved genome recovery from metagenomes through de-replication. ISME J 11:2864–2868. https://doi.org/10.1038/ismej.2017.126
77. Kanehisa M, Goto S. 2000. KEGG: Kyoto Encyclopedia of Genes and Genomes. Nucleic Acids Res 28:27–30. https://doi.org/10.1093/nar/28.1.27
78. Asnicar F, Thomas AM, Beghini F, Mengoni C, Manara S, Manghi P, Zhu Q, Bolzan M, Cumbo F, May U, Sanders JG, Zolfo M, Kopylova E, Pasolli E, Knight R, Mirarab S, Huttenhower C, Segata N. 2020. Precise phylogenetic analysis of microbial isolates and genomes from metagenomes using PhyloPhlAn 3.0. Nat Commun 11:2500. https://doi.org/10.1038/s41467-020-16366-7
79. Letunic I, Bork P. 2021. Interactive tree of life (iTOL) v5: an online tool for phylogenetic tree display and annotation. Nucleic Acids Res 49:W293–W296. https://doi.org/10.1093/nar/gkab301
80. Olson RD, Assaf R, Brettin T, Conrad N, Cucinell C, Davis JJ, Dempsey DM, Dickerman A, Dietrich EM, Kenyon RW, et al. 2023. Introducing the bacterial and viral bioinformatics resource center (BV-BRC): a resource combining PATRIC, IRD and ViPR. Nucleic Acids Res 51:D678–D689. https://doi.org/10.1093/nar/gkac1003
81. OksanenJ, Simpson G, Blanchet FG, KindtR, LegendreP, Minchin P, haraR, Solymos P, Stevens H. 2022. Vegan community ecology package version 2.6-2
82. Mallick H, Rahnavard A, McIver LJ, Ma S, Zhang Y, Nguyen LH, Tickle TL, Weingart G, Ren B, Schwager EH, Chatterjee S, Thompson KN, Wilkinson JE, Subramanian A, Lu Y, Waldron L, Paulson JN, Franzosa EA, Bravo HC, Huttenhower C. 2021. Multivariable association discovery in population-scale meta-omics studies. PLoS Comput Biol 17:e1009442. https://doi.org/10.1371/journal.pcbi.1009442

Downloaded from https://journals.asm.org/journal/msystems on 27 May 2026 by 203.255.190.49.